Compounds in the Infinitely Adaptive Series $Ba_p(Fe_2S_4)_q$: $Ba_9(Fe_2S_4)_8$

By J. T. Hoggins and H. Steinfink

Materials Science Laboratories, Materials Science and Engineering Program, The University of Texas at Austin, Austin, Texas 78712, USA

A complete crystal structure analysis of one member in the infinitely adaptive series, namely $Ba_9(Fe_2S_4)_8$, has been completed in the space group $P4/mnc$ with $a = 7.7758$ (10), $c = 44.409$ (8) Å and $Z = 2$. The Ba atoms are in strings along c and form an I-centered subcell, space group $I4/mmm$, with $a' = a$, $c' = \frac{1}{9}c$, and $Z' = 2$. The Fe atoms are tetrahedrally coordinated by S, and these tetrahedra share opposite edges to form infinite chains along c. The Fe_2S_4 subcell exhibits an I-centered space group $I4/mcm$, with $a'' = a$, $c'' = \frac{1}{8}c$, and $Z'' = 2$. The supercell space group $P4/mnc$ is the mathematical intersection of the two subcell space groups. The supercell reflections exhibited absences characteristic of a four-dimensional I-centered Bravais lattice. For those 679 reflections not space-group absent in the four-dimensional space group and with $F > \sigma(F)$, the crystallographic $R(F^2)$ is 0.12. For the complete set of 1954 reflections $R(F^2)$ is 0.14. The space-group analysis and structure principles have been extended to the other members in this series, and structures are proposed for all parity combinations of p and q.

Introduction

The system Ba—Fe—S contains an intermediate phase which can be designated $Ba_{1+x}Fe_2S_4$ or $Ba_p(Fe_2S_4)_q$ where p and q are integers and these compounds are part of a series to which the designation 'infinitely adaptive' was applied by Anderson (1973). Initially, one of these compounds, $Ba_9(Fe_2S_4)_8$, was synthesized and its characterization undertaken in these laboratories by Hong & Grey (1970, unpublished), and Reiff, Grey, Fan, Eliezer & Steinfink (1975). Recently, Grey reported crystal–chemical and structural data for several phases in this system including a detailed single-crystal X-ray diffraction study of $Ba_{10}(Fe_2S_4)_9$ (Grey, 1974, 1975). We report here a single-crystal X-ray diffraction study of the phase $Ba_9(Fe_2S_4)_8$ in which the relationship between the two incommensurate subcells and their space groups to the actual crystal structure and its space group is detailed. Similar problems have been encountered and solved in $(TTF)_7I_5$ (Johnson & Watson, 1977), $Mn_{15}Si_{26}$ (Knott, Mueller & Heaton, 1967) and $Rh_{17}Ge_{22}$ (Jeitschko & Parthé, 1967).

Experimental

The $Ba_9Fe_{16}S_{32}$ material for this analysis was prepared by reacting a mixture of BaS, Fe, and S powders with the stoichiometry 16:29:55. The mixture was packed into a capped carbon crucible and then sealed in a Vycor tube under a vacuum of 10^{-4} torr. This mixture was heated to 800°C for 3 d and slowly cooled at a rate of 300°C d^{-1}. X-ray diffraction powder patterns showed that the product was $Ba_9Fe_{16}S_{32}$, and pyrite. A needle-shaped crystal of dimensions $0.05 \times 0.08 \times 0.18$ mm was selected for single-crystal structure analysis.

The three-dimensional X-ray diffraction data can be indexed on the basis of a primitive tetragonal unit cell with $a = 7.7758$ (10), $c = 44.409$ (8) Å, $D_{calc} = 3.90$ g cm^{-3}, and $Z = 2$ for $Ba_9(Fe_2S_4)_8$. Two subcells are defined by very intense reflections occurring for $l = 9n$, $c' = 4.9341$ Å, and $l = 8n$, $c'' = 5.5509$ Å. The former is indicative of a Ba periodicity and the latter of an Fe_2S_4 unit periodicity (Grey, 1974). The lattice constants were determined from a least-squares refinement of precise 2θ measurements of 24 reflections between 27 and 95° at room temperature from a crystal mounted on a quarter-circle single-crystal diffractometer with the instrument set at 1° take-off angle and a 0.05° slit in front of the scintillation counter, and with Mo $K\alpha$ radiation, $\lambda_1 = 0.70926$ and $\lambda_2 = 0.71354$ Å.

Three-dimensional X-ray intensity data were collected with an automated diffractometer having the Weissenberg geometry and using a stationary-counter moving-crystal mode, and Mo $K\alpha$ radiation monochromatized by a graphite crystal. The crystal was aligned so that the a axis was parallel to the spindle axis of the machine. The procedure has been described in Lemley, Jenks, Hoggins, Eliezer & Steinfink (1976). Ten reciprocal-lattice layers were explored for $k \le h$ out to $(\sin \theta)/\lambda = 0.7035$ with 1954 independent reflections being measured. The intensities were transformed into structure factor amplitudes through the application of Lorentz–polarization and absorption corrections (transmission factors 0.162–0.560, $\mu_l = 121$

cm^{-1}). The structure factors for any symmetry-related reflections which were measured were averaged. The atomic scattering factors, including the real and imaginary corrections for anomalous scattering, were taken from Cromer & Mann (1968).

Some problems in the data collection were encountered because of the long c axis and the very large intensities of the subcell reflections. A compromise had to be made in the selection of the counter aperture size and scan angle so that individual reflections were resolved and the complete intensities of the subcell reflections were collected. This compromise caused some errors in the data, especially in those reflections whose l index differs from a very intense subcell reflection by 1.

The diffraction pattern of dual subcell systems invariably exhibits many systematic absences not related to space-group extinctions. We illustrate this phenomenon in Fig. 1 by a satellite intensity function. The subcell periodicities along c allow us to write the selection rule for intensities, $l = 8r + 9s$, where r and s are integers. This equation is used to form a table with entries $l = 8r + 9s \leq 63$. The three contours shown represent maximum F_o values for a given l. The solid contour represents $F_o > s(F_o)$, the dashed line represents $F_o \simeq F_c = 90$ and the dotted line is for $F_o \simeq F_c = 400$. The contour $F_o = 90$ illustrates very well the existence of a further subcell corresponding to the Fe—Fe repeat distance in the Fe_2S_4 subcell, $i.e.$ the $r = 2n$ are the intense reflections. Moreover, the satellite reflections exhibit the systematic absence hkl $(h,k,8r + 9s)$, $h + k + r + s = 2n$, indicative of a body-centered four-dimensional Bravais lattice. Some interesting concepts involving modulated structures and four-dimensional space have been developed by DeWolff (1974).

Space-group determination

The systematic absences for the complete data set are $hk0, h + k = 2n + 1$, $0kl, k + l = 2n + 1$, and $hhl, l = 2n + 1$, which indicate a probable space group of $P4/nnc$. The systematic absences for the Ba subcell, a

$= 7.7758, c' = 4.9341$ Å, $Z = 2$, characterized by $l = 9n$, are $hkl, h + k + l = 2n + 1$, consistent with $I4/mmm$ or the corresponding non-centrosymmetric groups. The systematic absences for the Fe_2S_4 subcell, $a = 7.7758, c'' = 5.5509$ Å, characterized by $l = 8n, Z = 2$, are $hkl, h + k + l = 2n + 1, 0kl, l = 2n + 1$, consistent with $I4/mcm$. Grey's data also exhibit the same systematic absences for the subcells. All compounds in this series are expected to display the Ba and Fe_2S_4 subcells with the same space groups. The space group of the supercells of a given structure in this series must be within the intersection of the two subcell space groups with the proper number of repeat translations. If the subcell space groups are expressed in terms of space-group generators, including sublattice translations, all equivalent positions for the supercell can be generated from each subcell. The positions in common, $i.e.$ the intersection, will form the highest possible symmetry of the supercell space group (Johnson & Watson, 1977). If the subcells are assumed to have the highest possible symmetries, $I4/mmm$ and $I4/mcm$, then a centrosymmetric supercell can be obtained if the symmetry centers, $4/m$ sites, of the subcells are superimposed. The subcell translations are 0,0,0; 1,0,0; 0,1,0; $\frac{1}{2},\frac{1}{2},1/2n$; where n is the number of subcells in the supercell.

An example of an equivalent point generation from the subcell space group $I4/mcm$ is illustrated by applying the c glide once and the translation $(\frac{1}{2},\frac{1}{2},1/2q)$ $(q - 1)$ times. Thus $x,y,z \to x, \bar{y}, 1/2q + z$ due to the c glide, and then the translation operations do the following:

$$(\frac{1}{2}, \frac{1}{2}, 1/2q)^{q-1}(x, \bar{y}, 1/2q + z) \to$$
$$(q - 1)/2 + x, (q - 1)/2 - y, \frac{1}{2} + z.$$

When q is even the resultant equipoint is $\frac{1}{2} + x, \frac{1}{2} - y, \frac{1}{2} + z$; for q odd the point is $x, \bar{y}, \frac{1}{2} + z$. The mirror operation from the space group $I4/mmm$ with the translation $(\frac{1}{2}, \frac{1}{2}, 1/2p)$ produces point $\frac{1}{2} + x, \frac{1}{2} - y, \frac{1}{2} + z$ for p odd and $x, \bar{y}, \frac{1}{2} + z$, for p even. The application of all symmetry operators present in the two subcell space groups will produce many points but only those which are common in both sets will describe the correct space group of the supercell.
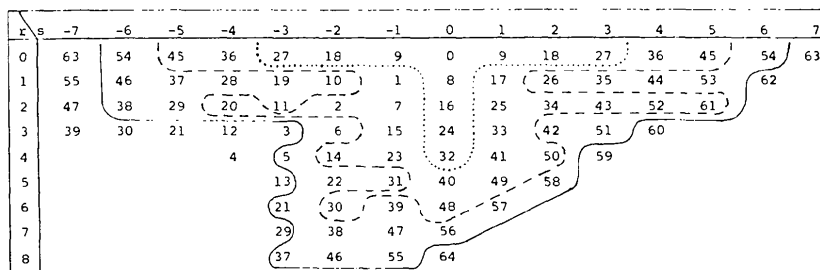

Fig. 1. Intensity map for $Ba_9(Fe_2S_4)_8$ based on the selection rule $l = 9s + 8r$. The tabulated values of l are contoured for maximum F_o value in a given layer line l.

The highest-symmetry space groups contained in the intersection for the various combinations of the stoichiometric coefficients p and q are:

p odd, q even P4/mnc example $Ba_9(Fe_2S_4)_8$

p even, q odd P4/mcc example $Ba_{10}(Fe_2S_4)_9$

p odd, q odd   I4/m   example $Ba_{21}(Fe_2S_4)_{19}$.

Grey's (1975) choice of space group P4/ncc for $Ba_{10}(Fe_2S_4)_9$, presumably because $h + k = 2n + 1$ for the $hk0$ set, is not correct. Those absences are due to the body-centered subcells. However, the choice of P4/mcc would cause only small changes in the structure.

Solution and refinement of the structure

For the Fe_2S_4 subcell, S tetrahedra which contain Fe and share opposite edges are formed when the Fe atom is on the $4(b)$ site and the S is on the $8(h)$ site of I4/mcm. A three-dimensional Patterson map calculated for this subcell gave $x \simeq 0.17$. Refinement of the subcell yielded $x = 0.162$ with an $R(F) = 0.21$. For the Ba subcell the Ba atom must be on the $2(a)$ site in I4/mmm. Refinement of this subcell yielded $R(F) = 0.29$.

This type of structure gives rise to many problems in least-squares refinements. These are due to numerical singularities in the matrix and the high correlations between subcell translations of related atoms. The weighting scheme is very important when a full-matrix least-squares program is used, and refinement was possible only when all reflections were used and weighted equally. Final refinements of the structure

were done with a modified version of a full-matrix least-squares program, GENLES.* The final value of $R(F^2)$ was 0.14 and $R(F) = 0.29$ for all 1954 reflections. $R(F) = 0.06$ for 320 reflections which have $F_c > 90$. A value of $F = 90$ corresponds roughly to those reflections which we observed by normal film techniques. There are 811 reflections which satisfy the conditions $h + k + r + s = 2n$ and $r + s < 7$ for which $R(F) = 0.14$. Within this group there are 679 reflections with $F > \sigma(F)$ and for these $R(F) = 0.12$. Anisotropic temperature coefficients were used for the Ba atoms and isotropic B values for the Fe and Se atoms. The maximum value of shift/σ for the final refinement was 1.1 while the average value was 0.2. The atomic parameters are listed in Table 1.

Attempts to refine the structure in the non-centrosymmetric space group P4nc were not successful. In addition to the previously discussed problems, there is a problem with the definition of the origin. Fixing the position of one Ba atom was not sufficient to define the origin for the Fe atoms. Consequently, the column of Fe atoms would drift with respect to the column of Ba atoms. This is caused by insufficient interactions between the two subcells. Least-squares refinement was possible only when the positions of one Ba and one Fe were fixed, i.e. define different origins for the two subcells. However, the relationship between the two positions is unknown. For these reasons no least-squares or Fourier refinement was possible in the non-centrosymmetric space group. The observed and calculated structure factors are given in Table 2.

Table 1. *Final atomic parameters and their standard deviations* ($\times 10^4$); $U_{12} = U_{13} = U_{23} = 0$

The temperature factor is:

$$\exp[-2\pi^2(U_{11}h^2a^{*2} + U_{22}k^2b^{*2} + U_{33}l^2c^{*2} + 2U_{12}hka^*b^* + 2U_{13}hla^*c^* + 2U_{23}klb^*c^*)].$$

	x	y	z	U_{11}	U_{22}	U_{33}
Ba(1)†	0	0	93 (2)	16 (2)	16 (2)	29 (5)
Ba(2)	0	0	1062 (1)	20 (1)	20 (1)	26 (3)
Ba(3)	0	0	2207 (1)	20 (1)	20 (1)	21 (2)
Ba(4)	0	0	3362 (1)	13 (1)	13 (1)	26 (3)
Ba(5)	0	0	4481 (2)	25 (2)	25 (2)	94 (6)
Fe(1)	0	½	310 (2)	12 (1)		
Fe(2)	0	½	920 (2)	15 (2)		
Fe(3)	0	½	1553 (2)	15 (2)		
Fe(4)	0	½	2177 (2)	14 (1)		
S(1)	3699 (15)	1964 (15)	0	8 (3)		
S(2)	1260 (13)	3084 (13)	609 (2)	23 (2)		
S(3)	3688 (11)	1815 (10)	1227 (2)	9 (2)		
S(4)	1672 (11)	3424 (11)	1884 (2)	13 (2)		
S(5)	3465 (17)	1534 (17)	¼	40 (5)		

† Occupancy of Ba(1) is 0.50.

Table 2. *Observed and calculated structure factors for* $Ba_9(Fe_2S_4)_8$

The column headings are k, l, $|F_o|$, and $|F_c|$. An asterisk denotes reflections which have $F_o < \sigma(F_o)$.

Discussion of the structure

A stereoscopic drawing illustrating one-half the unit cell is shown in Fig. 2 while Fig. 3 shows a projection down the [001] direction. The important interatomic distances are listed in Table 3. The S—S distances within a tetrahedron as well as intercolumn contacts vary from 3·38–4·17 Å. The structure consists of chains of edge-shared Fe—S tetrahedra along the c direction with the chain of Ba atoms in channels between the S atoms. The packing of these two chains causes considerable distortions from the 'ideal' positions in x,y,z for S and in z for Ba and Fe as listed in Table 4. The Fe—S distances vary from 2·21 to 2·32 Å. The ionic charges on independent Fe atoms calculated by the method of Hoggins & Steinfink (1976) also show considerable variation, from 2·54 to 3·20, with an average of 2·88 which is in good agreement with the stoichiometry. However, the individual charges should all be approximately the same since the Mössbauer spectrum shows only an averaged charge on Fe. The average Fe—S distance of 2·26 Å from the subcell refinement agrees very well with that expected from the Mössbauer spectrum. The large variation in Fe charges is probably indicative of errors in the structure solution. These errors are also evident in the S positions which

do not average to the value found in the subcell refinement.

The Ba—Ba distances along the chains vary from 4·30 to 5·13 Å. The coordination around the Ba atoms varies from 8 to 12; the coordination polyhedron goes from a square antiprism to a face-capped tetragonal prism. The Ba—S bond lengths in the square antiprism are 3·22 to 3·29 Å while in the face-capped tetragonal prism they are 3·28 to 4·13 Å. Ba(1) which is in the tetragonal prism is slightly off the mirror. This suggests that the ideal Ba position in $BaFe_2S_4$ is such that the coordination polyhedron about Ba is a square antiprism, i.e. $z(Ba) = 0·25$. This square-antiprism coordination is seen in various Ba—Fe—S compounds (Lemley et al., 1976). Thus, infinite columns of alter-

nately full and empty, face-sharing, square antiprisms are formed. However, the space group for this structure would be the non-centrosymmetric $I4$ rather than $I4/m$. Alternatively, if $z(Ba) = 0$ then infinite columns of face-capped tetragonal prisms are formed, as suggested by Grey (1974).

These two coordination possibilities suggest that the maximum Ba concentration in this system occurs when the Ba coordination alternates between these two types, i.e. square antiprisms share opposite faces with tetragonal prisms. This structure corresponds to the phase $Ba_4(Fe_2S_4)_3$ or $Ba_{1.333}Fe_2S_4$. We plotted Grey's (1974)
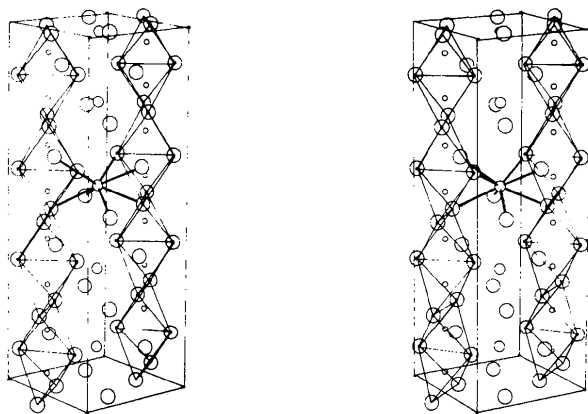

Fig. 2. Stereoscopic drawing showing approximately one half of the supercell. The $c/2$ axis is vertical and **a** is toward the viewer. Atoms at $x = 0$ and 1 are eliminated for clarity. The largest circles are S, the smaller circles are Ba, and the smallest are Fe.
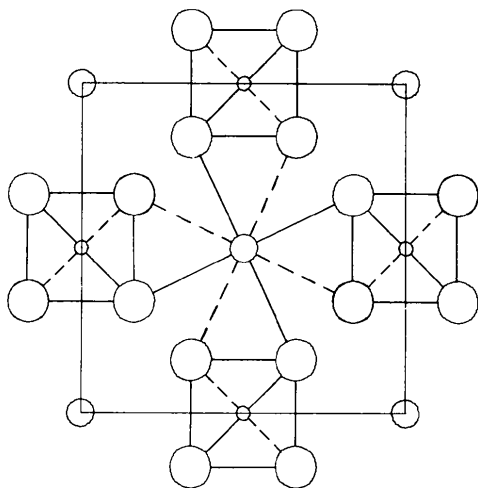

Fig. 3. The [001] projection of the supercell with S atoms in averaged positions showing S coordination around Ba and Fe atoms.

Table 3. Bond distances (Å) in $Ba_9(Fe_2S_4)_8$

2Fe(1)—S(1)	2·291 (10)	4Ba(1)—S(1)	3·282 (12)
2Fe(1)—S(2)	2·224 (11)	4Ba(1)—S(1)	4·051 (12)
2Fe(2)—S(2)	2·256 (10)	4Ba(1)—S(2)	3·459 (12)
2Fe(2)—S(3)	2·212 (9)	4Ba(2)—S(2)	3·279 (11)
2Fe(3)—S(3)	2·263 (9)	4Ba(2)—S(3)	3·280 (8)
2Fe(3)—S(4)	2·316 (9)	4Ba(3)—S(4)	3·291 (9)
2Fe(4)—S(4)	2·209 (9)	4Ba(3)—S(5)	3·222 (7)
2Fe(4)—S(5)	2·215 (15)	4Ba(4)—S(3)	3·240 (9)
Fe(1)—Fe(1)	2·751 (17)	4Ba(4)—S(4)	3·065 (9)
Fe(1)—Fe(2)	2·710 (13)	4Ba(5)—S(1)	3·452 (10)
Fe(2)—Fe(3)	2·809 (11)	4Ba(5)—S(2)	3·292 (10)
Fe(3)—Fe(4)	2·773 (12)	4Ba(5)—S(3)	4·129 (10)
Fe(4)—Fe(4)	2·868 (15)		

Table 4. Displacements (Å) from 'ideal' positions $(\times 10^2)$

	Δz		Δx	Δy	Δz
Ba(1)	41	Fe(3)			−4
Ba(2)	−22	Fe(4)			−5
Ba(3)	−7	S(1)	25	25	0
Ba(4)	13	S(2)	−28	−22	−7
Ba(5)	16	S(3)	23	16	−10
Fe(1)	−1	S(4)	8	3	−4
Fe(2)	−8	S(5)	7	−7	0

Table 5. Approximate structures for the series $Ba_p(Fe_2S_4)_q$

$P4/mnc$: p odd, q even
Ba	4(e)	$z \simeq 0, 1/p, 2/p \cdots < \frac{1}{2}$
Fe	8(f)	$z \simeq 1/4q, 3/4q, \cdots < \frac{1}{2}$
S(1)	16(i)	$x \simeq 0·34; y \simeq 0·16; z \simeq 0, 1/q, \cdots \leq \frac{1}{4}$
S(2)	16(i)	$x \simeq 0·16; y \simeq 0·34; z \simeq 1/2q, 3/2q, \cdots < \frac{1}{4}$

$P4/mcc$: p even, q odd
Ba(1)	4(g)	$z \simeq 0, 1/p, \cdots \leq \frac{1}{4}$
Ba(2)	4(h)	$z \simeq 1/2p, 3/2p, \cdots < \frac{1}{4}$
Fe	8(i)	$z \simeq 1/4q, 3/4q, \cdots < \frac{1}{2}$
S(1)	16(n)	$x \simeq 0·34; y \simeq 0·16; z \simeq 0, 1/q, \cdots < \frac{1}{4}$
S(2)	16(n)	$x \simeq 0·16; y \simeq 0·34; z \simeq 1/2q, 3/2q, \cdots < \frac{1}{4}$

$I4/m$: p odd, q odd
Ba	4(e)	$z = 0, 1/p, 2/p, \cdots < \frac{1}{2}$
Fe	8(q)	$z = 1/4q, 3/4q, \cdots < \frac{1}{2}$
S(1)	16(i)	$x \simeq 0·34; y \simeq 0·16; z \simeq 0, 1/q, \cdots < \frac{1}{4}$
S(2)	16(i)	$x \simeq 0·16; y \simeq 0·34; z \simeq 1/2q, 3/2q, \cdots < \frac{1}{4}$

data for the Fe_2S_4 subcell c'' axis *versus* Ba concentration and by extrapolation we obtain $c'' = 5.88$ Å. Thus $c = 17.64$ Å and the Ba—Ba repeat distance is 4.41 Å in this phase. Attempts to prepare those two compounds, $BaFe_2S_4$ and $Ba_{1.333}Fe_2S_4$, to confirm the above are currently underway.

The basic structure principles for $Ba_9Fe_{16}S_{32}$ can be extended to postulate the approximate structures of all other members of the series $Ba_p(Fe_2S_4)_q$ where p and q are integers (Table 5).

It had been proposed that this system presents a model system for testing current theories which postulate that quenched high-temperature structures represent frozen 'quantum states' of the periodic thermal vibrations of the atoms (Grey, 1974). We made a study of the X-ray powder diffraction pattern at temperatures up to 535°C. Only the normal thermal expansion was observed up to approximately 450°C. Above this temperature the sample began to decompose slowly. No phase transformations were observed.

The authors gratefully acknowledge the research support provided by a grant from The Robert A. Welch Foundation, Houston, Texas.

References

ANDERSON, J. S. (1973). *J. Chem. Soc. Dalton*, pp. 1107–1115.
CROMER, D. T. & MANN, J. B. (1968). *Acta Cryst.* A24, 321–324.
DEWOLFF, P. M. (1974). *Acta Cryst.* A30, 777–785.
GREY, I. (1974). *J. Solid State Chem.* 11, 128–134.
GREY, I. (1975). *Acta Cryst.* B31, 45–48.
HOGGINS, J. T. & STEINFINK, H. (1976). *Inorg. Chem.* In the press.
JEITSCHKO, W. & PARTHÉ, E. (1967). *Acta Cryst.* 22, 417–430.
JOHNSON, C. K. & WATSON, C. R. JR (1977). *J. Chem. Phys.* To be published.
KNOTT, H. W., MUELLER, M. H. & HEATON, L. (1967). *Acta Cryst.* 23, 549–555.
LEMLEY, J. T., JENKS, J. M., HOGGINS, J. T., ELIEZER, Z. & STEINFINK, H. (1976). *J. Solid State Chem.* 16, 117–128.
REIFF, W. M., GREY, I., FAN, A., ELIEZER, Z. & STEINFINK, H. (1975). *J. Solid State Chem.* 13, 32–40.

Activated Cyclophosphamide Anticancer Drugs: Molecular Structure of 4-Hydroperoxycyclophosphamide

BY ARTHUR CAMERMAN AND H. WARREN SMITH

Departments of Medicine and Pharmacology, University of Washington, Seattle, Washington 98195, USA

AND NORMAN CAMERMAN

Department of Biochemistry, University of Toronto, Toronto, Ontario, Canada

4-Hydroperoxycyclophosphamide is an active cytostatic agent closely related to an active metabolite of the antitumor drug cyclophosphamide. $C_7H_{15}Cl_2N_2O_4P$, monoclinic, $P2_1/c$; $a = 14.229$ (4), $b = 7.706$ (3), $c = 11.891$ (3) Å, $\beta = 103.06$ (2)°, $Z = 4$, $D_x = 1.533$ g cm^{-3}; $T = -5$°C. The structure was solved by direct methods and refined by full-matrix least-squares methods to $R = 0.055$ for 1957 observed reflections. The configuration at the P atom is phosphoryl O axial and dialkyamino group equatorial. The peroxide group attached to C(4) is axial and is thus *cis* to the phosphoryl O.

Introduction

Cyclophosphamide (CPA) (Fig. 1), an antitumor alkylating agent, is one of the most widely used drugs in the treatment of many types of cancer. Though it is an effective antineoplastic agent against many tumors, CPA has virtually no cytotoxic activity against mammalian cell cultures (Arnold, Bourseaux & Brock, 1958); *in vivo* pharmacological activity requires conversion of CPA to alkylating substances by the mixed function oxidase system of liver microsomes (Brock & Hohorst, 1963; Cohen & Jao, 1970). It is becoming increasingly clear that mono-oxidation at C(4) is responsible for activation of CPA with the first step being production of 4-hydroxycyclophosphamide (HCPA) (Hohorst, Ziemann & Brock, 1971; Hill, Laster &